Int J Clin Exp Pathol 2019;12(8):2826-2836
www.ijcep.com /ISSN:1936-2625/IJCEP0096009

Original Article

Effect of hydrogel stiffness on morphology and gene expression pattern of CD44^{high} oral squamous cell carcinoma cells

Hideo Shigeishi[1], Sho Yokoyama[2], Hiroshi Murodumi[2], Miyuki Sakuma[2], Hiroki Kato[2], Koichiro Higashikawa[2], Masaaki Takechi[2], Kouji Ohta[1], Masaru Sugiyama[1]

[1]Department of Public Oral Health, Program of Oral Health Sciences, Graduate School of Biomedical and Health Sciences, Hiroshima University, 1-2-3 Kasumi, Minami-ku, Hiroshima 734-8553, Japan; [2]Department of Oral and Maxillofacial Surgery, Program of Dentistry, Graduate School of Biomedical and Health Sciences, Hiroshima University, 1-2-3 Kasumi, Minami-ku, Hiroshima 734-8553, Japan

Received April 24, 2019; Accepted May 28, 2019; Epub August 1, 2019; Published August 15, 2019

Abstract: The stiffness of extracellular matrix (ECM) has been associated with tumor growth, phenotypic plasticity, and invasion through modulation of the intracellular signaling pathway. However, the effect of ECM stiffness on oral cancer stem cells (CSCs) has not been fully elucidated. Therefore, we preliminarily investigated changes in phenotype and gene expression in CD44 positive-oral squamous cell carcinoma (OSCC) cells (i.e., CD44^{high} OM-1 cells) that were cultured on laminin-coated hydrogel with various degrees of stiffness. Mesenchymal-like morphology was observed when cells were cultured on 4.0 kPa laminin-coated hydrogel; amoeboid-like morphology was observed when cells were cultured on 1.0 kPa and 0.5 kPa laminin-coated hydrogel. These results indicated that CD44^{high} OM-1 cells underwent mesenchymal to amoeboid transition (MAT) when cultured on laminin-coated softer hydrogel. E-cadherin and ESA mRNA expression levels were significantly reduced in CD44^{high} OM-1 cells cultured on 0.5 and 1.0 kPa laminin-coated hydrogel, compared with their levels in control cells cultured in laminin-coated dishes. Significant changes in CD44 mRNA expression were not found in CD44^{high} OM-1 cells that were cultured on different stiff hydrogels, compared with expression in control cells. Microarray analysis revealed that expression of cofilin, an intracellular actin-modulating protein, was increased by 8.19-fold in amoeboid-like CD44^{high} OM-1 cells, compared with mesenchymal-like CD44^{high} OM-1 cells; this suggested that cofilin was associated with MAT in CD44^{high} OSCC cells. Further studies are needed to clarify the relationship between cofilin and invasion ability in CD44^{high} amoeboid-like OSCC cells.

Keywords: Cancer stem cells, oral squamous cell carcinoma, CD44, mesenchymal to amoeboid transition, extracellular matrix

Introduction

CD44 positive-oral squamous cell carcinoma (OSCC) cells reportedly demonstrate characteristics of cancer stem cells (CSCs), such as self-renewal ability and high tumor-initiating capacity [1]. Importantly, CD44^{high} OSCC cells have been shown to exhibit phenotypic plasticity, such as mesenchymal to epithelial transition (EMT) [2]. We previously reported that CD44^{high}/ESA^{low} OSCC cells are involved in resistance to chemotherapy-induced apoptosis, which may cause cancer recurrence [3-5]. CD44^{high}/ESA^{low} cells with mesenchymal properties exhibited strong resistance to 5-fluorouracil (5-FU)-induced apoptosis, in addition to high dihydropyrimidine dehydrogenase expression [3]. In addition, we previously reported that CD44^{high} OSCC cells with mesenchymal characteristics showed CSC properties that were mediated in a GSK3β-dependent manner [6, 7]. Therefore, we suspected that surviving mesenchymal-like CSCs after chemotherapy may be involved in recurrence by activation of GSK3β, resulting in worse outcomes for OSCC patients.

In the cancer microenvironment, cancer cells are surrounded by stromal cells, such as fibroblasts, immune cells, vascular cells, and extra-

cellular matrix (ECM). In addition, cancer cells are exposed to various types of mechanical stresses, such as cell-cell and cell-ECM stress, compression stress, and shear stress [8]. Cell surface receptors in the integrin family play important roles in mediating interactions between cells and ECM [9]. Mechanical stress in the tumor matrix can be sensed by integrin receptors, resulting in mechanical force transmission and biochemical signal transduction across the cell membrane [10, 11]. Therefore, ECM stiffness is associated with tumor growth, phenotypic plasticity, and invasion by modulation of the intracellular signaling pathway [11-14], and may be associated with altered biologic features (e.g., changes in gene expression, cell signaling pathways, and morphologic features) in CSCs. However, the effect of ECM stiffness on CSC properties in oral cavity cancers has not been fully elucidated. Therefore, we preliminarily investigated changes in phenotype and gene expression in CD44^{high} OM-1 cells that were cultured on hydrogel with various degrees of stiffness.

Materials and methods

Cell culture and fluorescence-activated cell sorting

The human OSCC cell line, OM-1, was cultured in Dulbecco's modified Eagle's medium (DMEM) with glucose, L-glutamine, sodium pyruvate, and sodium bicarbonate (Merck KGaA, Darmstadt, Germany) supplemented with 1% penicillin/streptomycin (Thermo Fisher Scientific, Waltham, MA, USA) and 10% heat-inactivated fetal bovine serum under 5% CO_2 in air at 37°C. Cells were released into suspension using Accutase (Nakalai Tesque, Kyoto, Japan), and were stained using anti-CD44PE-conjugated antibody (BD Pharmingen, San Diego, CA, USA). 7-AAD was used to exclude dead cells. Samples were assayed using a Becton Dickenson FACSCalibur™ (BD Pharmingen) and CD44^{high} OM-1 cells were sorted using Becton Dickenson FACSAria equipment, in accordance with the method used in our previous experiment [6].

Softwell assay

To investigate the effects of matrix stiffness on CD44^{high} OM-1 cells, 12-well Matrigen Softwell® plates (Matrigen Life Technologies, Brea, CA, USA) with eight levels of stiffness (50 kPa, 25 kPa, 12 kPa, 8.0 kPa, 4.0 kPa, 2.0 kPa, 1.0 kPa, and 0.5 kPa) were used in this study. Two micrograms of laminin-5 (Repro CELL, Beltsville, MD, USA) per well were used as extracellular matrix protein, because laminin-5 is thought to play a vital role in tumor growth and migration [15]. After preparation of laminin-coated hydrogel for 3 h at room temperature, cells were seeded at 1.0×10^4 cells per well.

RT-PCR analysis

RNA was extracted using an RNAeasy Micro kit (Qiagen, Hilden, Germany) and 1 μg of total RNA was subjected to cDNA synthesis using a High Efficient Reverse Transcription Kit (Toyobo Life Science, Osaka, Japan). Semi-quantitative RT-PCR was performed with 10X PCR buffer, dNTPs, Taq DNA polymerase (Toyobo Life Science), and primers. Amplifications were performed with 30 cycles of denaturing at 95°C for 30 seconds, then annealing at 57°C for 30 seconds and extension at 72°C for 60 seconds. PCR products were separated by electrophoresis on 2% agarose gels and visualized by staining with ethidium bromide. The primer sequences were as follows. Vimentin: 5'-CCCTCACCTGTGAAGTGGAT-3' (sense), 5'-GACGAGCCATTTCCTCCTTC-3' (antisense); E-cadherin: 5'-GAACGCATTGCCACATACAC-3' (sense), 5'-AGCACCTTCCATGACAGACC-3' (antisense); ESA: 5'-CAATGCAGGGTCTAAAAGCTG-3' (sense), 5'-CACCCATCTCCTTTATCTCAGC-3' (antisense); CD44: 5'-TCCAACACCTCCCAGTATGACA-3' (sense), 5'-GGCAGGTCTGTGACTGATGTACA-3' (antisense) and G3PDH: 5'-GTGAACCATGAGAAGTATGACAAC-3' (sense), 5'-ATGAGTCCTTCCACGATACC-3' (antisense). Kodak Digital Science 1D Software (Eastman Kodak, Rochester, NY, USA) was used for densitometric scanning of the PCR bands. mRNA expression levels of vimentin, E-cadherin, ESA, and CD44 were normalized to the internal control (G3PDH) signals by calculating the ratio of the band densities of vimentin, E-cadherin, ESA, and CD44 to the control signal in each sample.

Immunofluorescence

Cells were fixed with 4% paraformaldehyde in phosphate-buffered saline (PBS) for 20 minutes, then permeabilized using 0.2% Triton-X in

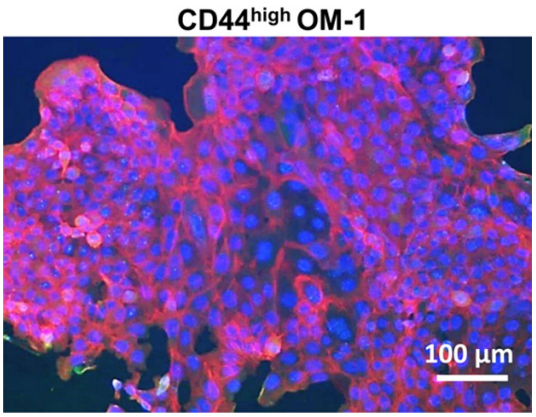

Figure 1. Immunofluorescence localization of F-actin and vimentin in CD44high OM-1 cells. Fluorescence immunostaining of F-actin (red) and vimentin (green), as well as nuclear stain with 4',6-diamidino-2-phenylindole (DAPI) (blue). F-actin and vimentin expression were found in the cytoplasm in CD44high OM-1 cells.

PBS for 5 minutes. Next, they were incubated with an anti-vimentin mouse monoclonal antibody (MONOSAN, Uden, Netherlands) (diluted 1:100) in PBS with 1% bovine serum albumin at 4°C. Binding of the anti-vimentin mouse monoclonal antibody was revealed by incubation with Alexa Fluor® 488 goat anti-mouse antibody (1:1000) for 60 minutes at room temperature. Alexa Fluor 568 phalloidin (Thermo Fisher Scientific) (diluted 1:500) was used to stain F-actin. Slides were rinsed in PBS, then mounted in Dapi-Fluoromount-G (Southern Biotech, Birmingham, AL, USA) and examined using a Fluorescence Microscope (BIOREVO BZ-9000 series; KEYENCE, Kyoto, Japan).

Microarray analysis

Briefly, total RNA was reverse-transcribed to synthesize cRNA using the GeneChip® WT PLUS Reagent Kit (Thermo Fisher Scientific). After synthesizing cDNA from cRNA, the sense-stranded DNA was fragmented and biotinylated. Single-Strand cDNA was hybridized on a Clariom S Human MicroArray (Thermo Fisher Scientific) at 45°C for 16 h using a GeneChip Hybridization Oven 640 (Thermo Fisher Scientific). After hybridization, the arrays were washed and stained by a GeneChip™ Expression, Wash and Stain Kit (Thermo Fisher Scientific). Finally, data were collected using the GeneChip™ Scanner 3000 7G (Thermo Fisher Scientific). Data were analyzed with Expression Console Software version 1.4 (Thermo Fisher Scientific) and the Signal Space Transformation-Robust Multi-array Average was used for gene level analysis. Data analyses were performed using Expression Console™ Software 1.4.1 (Thermo Fisher Scientific). To classify the functional roles of differentially expressed genes, Gene Ontology analysis was performed using the Database for Annotation, Visualization, and Integrated Discovery v6.8 [16].

Statistical methods

Statistical analysis of *in vitro* experiments was performed using Dunnett tests to compare the control group with the other groups. *P* values less than 0.05 were considered significant.

Results

Morphological change in CD44high OM-1 cells

CD44high OM-1 cells exhibited an epithelial-like phenotype when they were cultured on plastic dishes (**Figure 1**). To investigate the effect of stiffness mimicking that of biological tissues on morphological changes in cancer stem-like cells, CD44high OM-1 cells were cultured on laminin-coated hydrogel with various degrees of stiffness. CD44high OM-1 cells cultured on 50 kPa laminin-coated hydrogel exhibited epithelial-like phenotypes (**Figure 2A**). Nearly all CD44high OM-1 cells became elongated cells when cultured on 12 kPa laminin-coated hydrogel (**Figure 2B**); they exhibited loss of cell-cell adhesion when cultured on 8.0 kPa laminin-coated hydrogel (**Figure 2C**). Mesenchymal-like cells were observed when cells were cultured on 4.0 kPa laminin-coated hydrogel (**Figure 2D**). Importantly, amoeboid-like cells were observed when cells were cultured on 1.0 and 0.5 kPa laminin-coated hydrogel (**Figure 2E** and **2F**). Amoeboid-like CD44high OM-1 cells exhibited cellular blebs (i.e., spherical cellular protrusions) (**Figure 2E**). Vimentin expression was not observed when cells were cultured on 1.0 and 0.5 kPa laminin-coated hydrogel (**Figure 2E** and **2F**).

E-cadherin, ESA, vimentin, and CD44 mRNA expression level in CD44high OM-1 cells

Next, we examined mRNA expression levels of epithelial markers (E-cadherin and ESA), a mes-

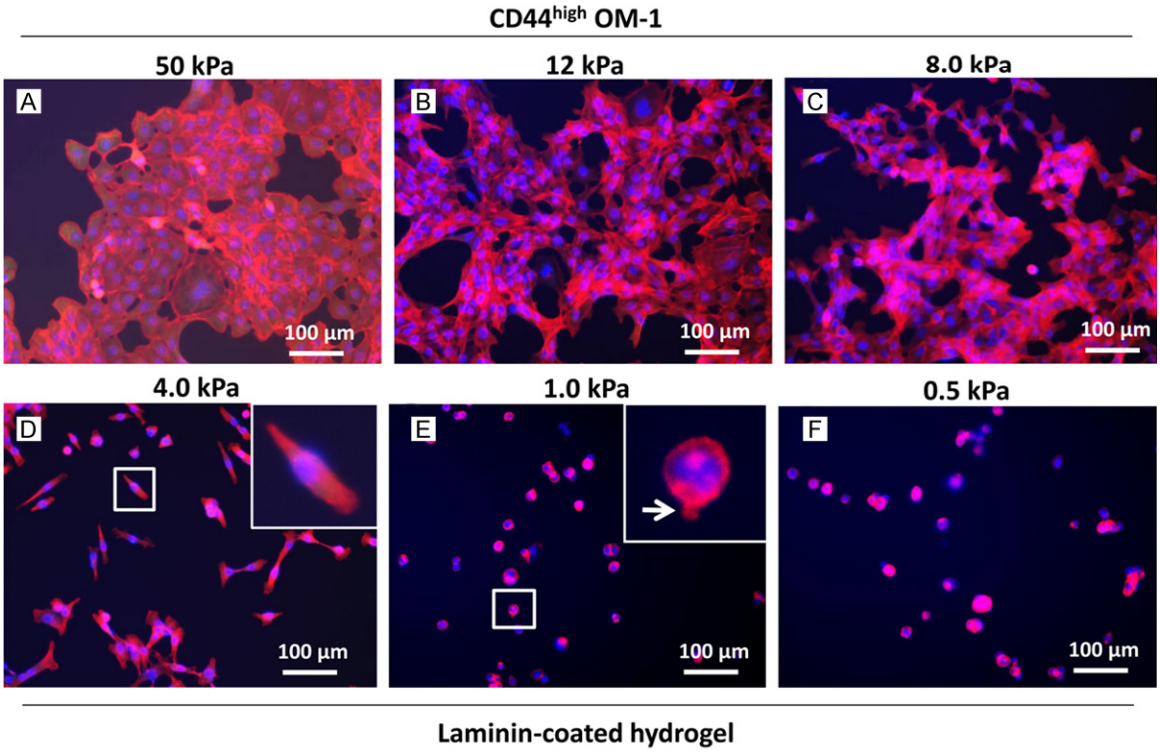

Figure 2. Immunofluorescence localization of F-actin and vimentin in CD44high OM-1 cells cultured on laminin-coated hydrogel with various degrees of stiffness. Fluorescence immunostaining of F-actin (red) and vimentin (green), as well as nuclear stain with 4',6-diamidino-2-phenylindole (DAPI) (blue). A. CD44high OM-1 cells were cultured on 50 kPa laminin-coated hydrogel. B. CD44high OM-1 cells were cultured on 12 kPa laminin-coated hydrogel. C. CD44high OM-1 cells were cultured on 8.0 kPa laminin-coated hydrogel. D. CD44high OM-1 cells were cultured on 4.0 kPa laminin-coated hydrogel. Mesenchymal-like cells were observed. E. CD44high OM-1 cells were cultured on 1.0 kPa laminin-coated hydrogel. Amoeboid-like cells exhibited cellular blebs (arrow). F. CD44high OM-1 cells were cultured on 0.5 kPa laminin-coated hydrogel.

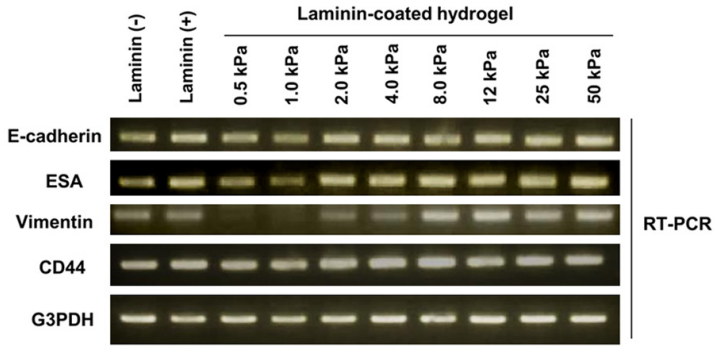

Figure 3. mRNA expression levels of E-cadherin, ESA, vimentin, and CD44, as determined by RT-PCR. mRNA expression levels of E-cadherin, ESA, vimentin, and CD44 were examined by RT-PCR in CD44high OM-1 cells cultured on laminin-coated hydrogel with various degrees of stiffness.

enchymal marker (vimentin) and CD44 by RT-PCR (**Figure 3**). E-cadherin and ESA mRNA expression levels were significantly reduced in CD44high OM-1 cells cultured on 0.5 and 1.0 kPa laminin-coated hydrogel, compared with CD44high OM-1 cells cultured on laminin-coated plastic dishes (control cells) (**Figure 4A** and **4B**). Vimentin mRNA expression levels were significantly reduced in CD44high OM-1 cells cultured on 1.0 and 0.5 kPa laminin-coated hydrogel, compared with control cells (**Figure 4C**). Conversely, vimentin mRNA expression was significantly increased in CD44high OM-1 cells cultured on 8.0, 12, 25, and 50 kPa laminin-coated hydrogel, compared with control cells (**Figure 4C**). A significant change in CD44 mRNA expression was not observed in CD44high OM-1 cells cultured on hydrogels with various degrees of stiffness, compared with control cells (**Figure 4D**).

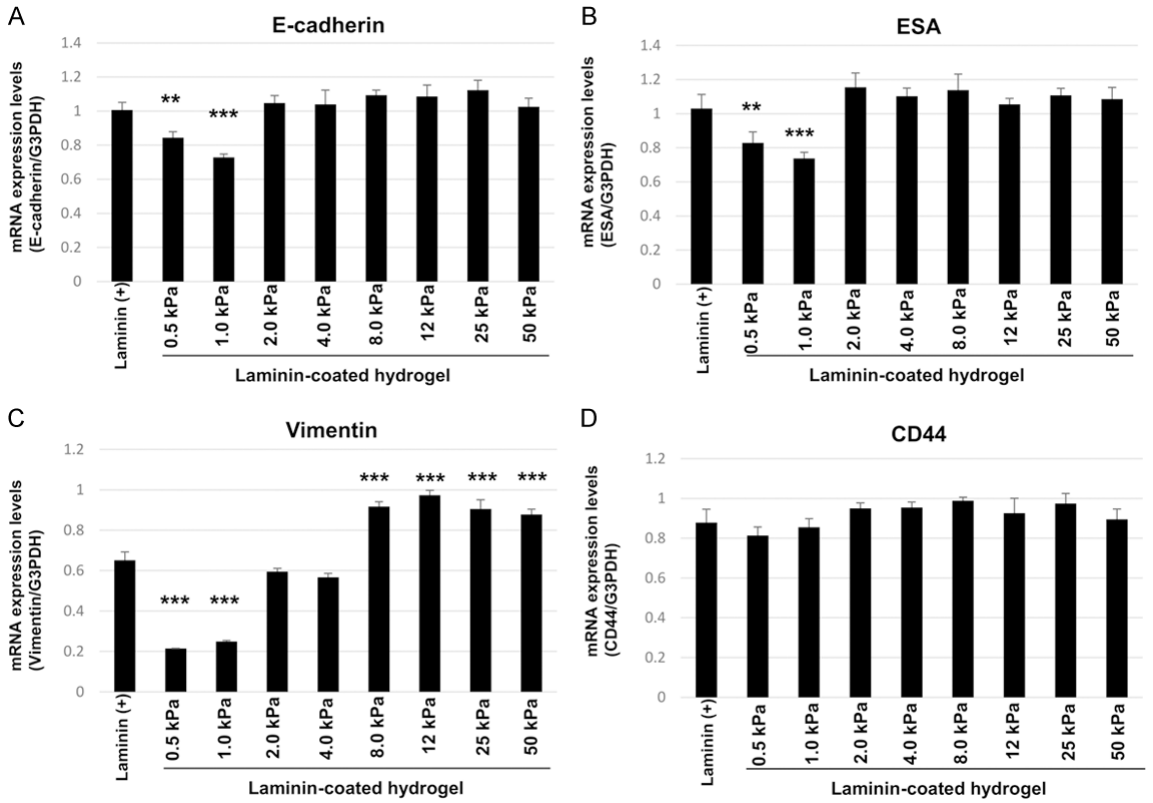

Figure 4. Relative mRNA expression levels of E-cadherin, ESA, vimentin, and CD44. The band density ratios of E-cadherin, ESA, vimentin, and CD44 to the control signal were calculated in each sample. (A) E-cadherin, (B) ESA, (C) vimentin, and (D) CD44. (Statistical significance levels of $P < 0.01$ and $P < 0.001$ are indicated by ** and ***, respectively).

Table 1. Summary of upregulated genes (> 5.0-fold increase) in amoeboid-like CD44^{high} cells

Gene symbol	Description	Fold change
C16orf52	chromosome 16 open reading frame 52	25.48
FOS	FBJ murine osteosarcoma viral oncogene homolog	11.00
DHRS9	dehydrogenase/reductase (SDR family) member 9	9.00
CFL1	cofilin 1	8.19
GABRE: MIR224: MIR452	gamma-aminobutyric acid (GABA) A receptor, epsilon: microRNA 224: microRNA 452	8.13
SYTL2	synaptotagmin-like 2	7.24
BHLHE41	basic helix-loop-helix family, member e41	7.02
S100A7	S100 c	6.74
CCL22	chemokine (C-C motif) ligand 22	6.47
TRIM31	tripartite motif containing 31	6.36
RFX3	Memczak2013 ALT_ACCEPTOR, ALT_DONOR, coding, INTERNAL, intronic best transcript NM_002919	6.29
KRT13	keratin 13, type I	6.09
CFB	complement factor B	5.86
PSCA	prostate stem cell antigen	5.70
RDH10	retinol dehydrogenase 10 (all-trans)	5.68
NAPEPLD	N-acyl phosphatidylethanolamine phospholipase D	5.68
S100A7A	S100 calcium binding protein A7A	5.65
PLEKHH1	pleckstrin homology domain containing, family H (with MyTH4 domain) member 1	5.24
AHCYL2	adenosylhomocysteinase-like 2	5.20
TNFAIP2	tumor necrosis factor, alpha-induced protein 2	5.09
TMPRSS4	transmembrane protease, serine 4	5.01

Table 2. Summary of downregulated genes (< 0.2-fold decrease) in amoeboid-like CD44^{high} cells

Gene symbol	Description	Fold change
CTGF	connective tissue growth factor	0.092
SERPINB2	serpin peptidase inhibitor, clade B (ovalbumin), member 2	0.096
TNF	tumor necrosis factor	0.100
THBS1	thrombospondin 1	0.114
SPOCK1	sparc/osteonectin, cwcv and kazal-like domains proteoglycan (testican) 1	0.115
IL6	interleukin 6	0.120
DEFB103A	defensin, beta 103A	0.121
SPRR1A	small proline-rich protein 1A	0.127
MSN	moesin	0.129
GAL	galanin/GMAP prepropeptide	0.134
CTSV	cathepsin V	0.140
DEFB103A: DEFB103B	defensin, beta 103A: defensin, beta 103B	0.149
FAM25A	family with sequence similarity 25, member A	0.154
MRPL55	mitochondrial ribosomal protein L55	0.164
SRGN	serglycin	0.170
COMMD4	COMM domain containing 4	0.173
ALKBH7	alkB homolog 7	0.174
TIMM8A	translocase of inner mitochondrial membrane 8 homolog A	0.179
NUAK2	NUAK family, SNF1-like kinase, 2	0.179
TIMM10	translocase of inner mitochondrial membrane 10 homolog	0.183
TMEM141	transmembrane protein 141	0.187
SPRR3	small proline-rich protein 3	0.189
TUBA4A	tubulin, alpha 4a	0.190
NDUFS7	NADH dehydrogenase (ubiquinone) Fe-S protein 7	0.190
CCDC80: LINC01279	coiled-coil domain containing 80 : long intergenic non-protein coding RNA 1279	0.191
TMEM109	transmembrane protein 109	0.196
WLS	wntless Wnt ligand secretion mediator	0.197
TRHDE	thyrotropin-releasing hormone degrading enzyme	0.198
CXCL10	chemokine (C-X-C motif) ligand 10	0.198
EMG1	EMG1 N1-specific pseudouridine methyltransferase	0.198

Microarray analysis of amoeboid-like CD44^{high} cells and mesenchymal-like CD44^{high} cells

To clarify differences in gene expression patterns between mesenchymal-like CD44^{high} cells and amoeboid-like CD44^{high} cells, we compared gene expression between CD44^{high} OM-1 cells cultured on 0.5 kPa laminin-coated hydrogel (i.e., amoeboid-like CD44^{high} cells) and those cultured on 4.0 kPa laminin-coated hydrogel (i.e., mesenchymal-like CD44^{high} cells). A total of 1874 genes were differentially expressed in amoeboid-like CD44^{high} cells, compared with those expressed in mesenchymal-like CD44^{high} cells. Of these genes, 847 genes were upregulated (> 2-fold increase), while 1027 genes were downregulated (< 0.5-fold decrease). The upregulated (> 5-fold increase) and downregulated (< 0.2-fold decrease) genes are summarized in **Tables 1** and **2**. The chromosome 16 open reading frame 52 gene showed > 25.0-fold increased expression in amoeboid-like CD44^{high} cells, compared with its expression in mesenchymal-like CD44^{high} cells. In addition, cofilin, an intracellular actin-modulating protein, showed an 8.19-fold increase in CD44^{high} amoeboid-like cells, compared with its expression in mesenchymal-like CD44^{high} cells. In contrast, connective tissue growth factor and serpin peptidase inhibitor, clade B, member 2 showed > 10-fold decreased expression in amoeboid-like CD44^{high} cells compared with mesenchymal-like CD44^{high} cells.

Gene ontology analysis of microarray data was performed to identify functional annotations

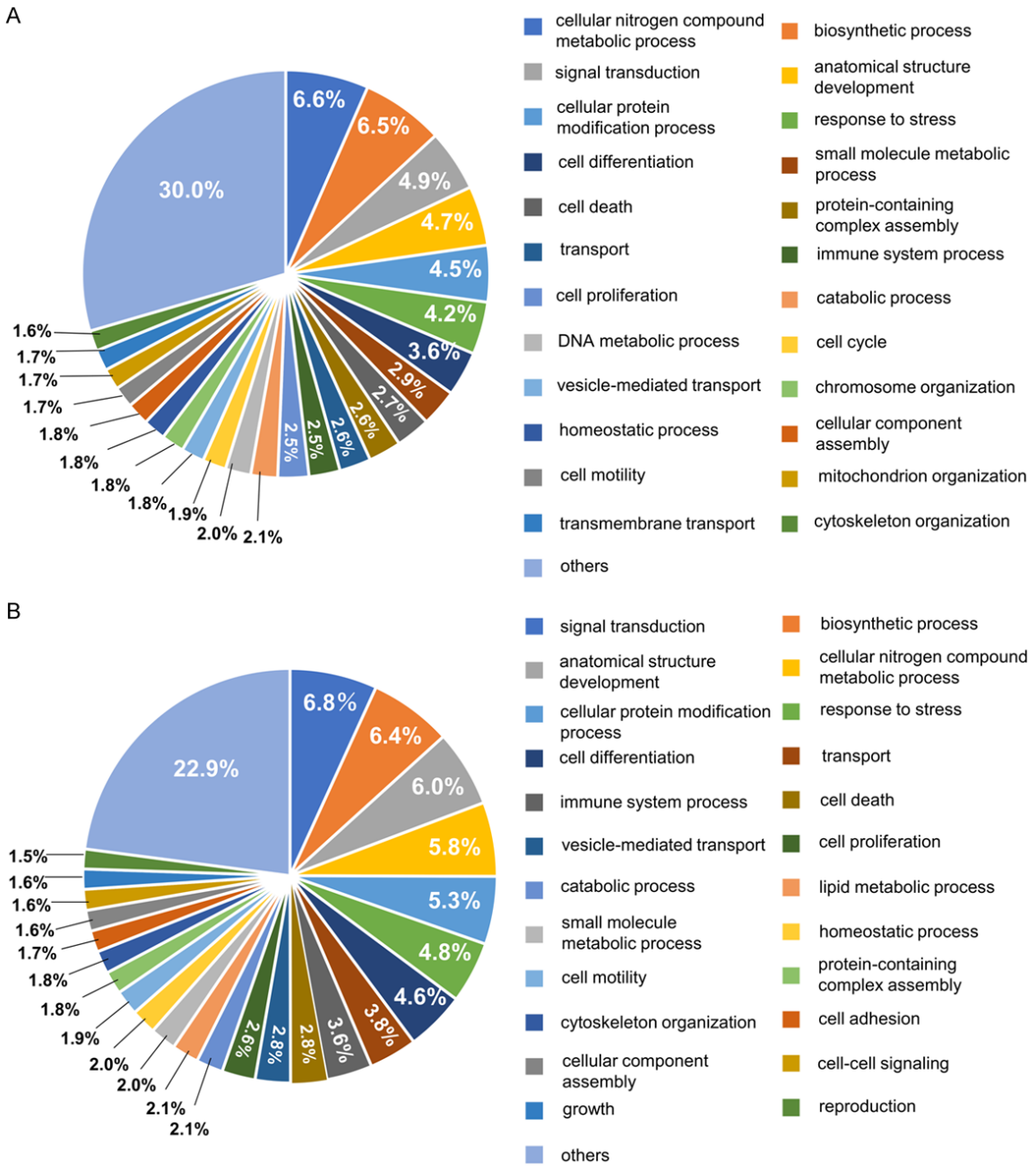

Figure 5. Gene Ontology enrichment analysis, focused on biologic processes. A. Enriched Gene Ontology terms among upregulated (> 2-fold increase) genes in amoeboid-like CD44^{high} cells, compared with mesenchymal-like CD44^{high} cells. B. Enriched Gene Ontology terms among downregulated (< 0.5-fold decrease) genes in amoeboid-like CD44^{high} cells, compared with mesenchymal-like CD44^{high} cells.

(e.g., biologic processes, molecular functions, and cellular components) of > 2-fold upregulated or < 0.5-fold downregulated genes in amoeboid-like CD44^{high} cells, compared with mesenchymal-like CD44^{high} cells. With respect to biological processes, multiple GO terms (e.g., signal transduction, biosynthetic process, anatomical structure development, cellular nitrogen compound metabolic process, cellular protein modification process, response to stress, and cell differentiation) were found to include both up- and downregulated genes (**Figure 5**). With respect to cellular components, the most abundant GO terms upregulated genes and downregulated genes were protein-containing complex and cytoplasm, respectively (**Figure**

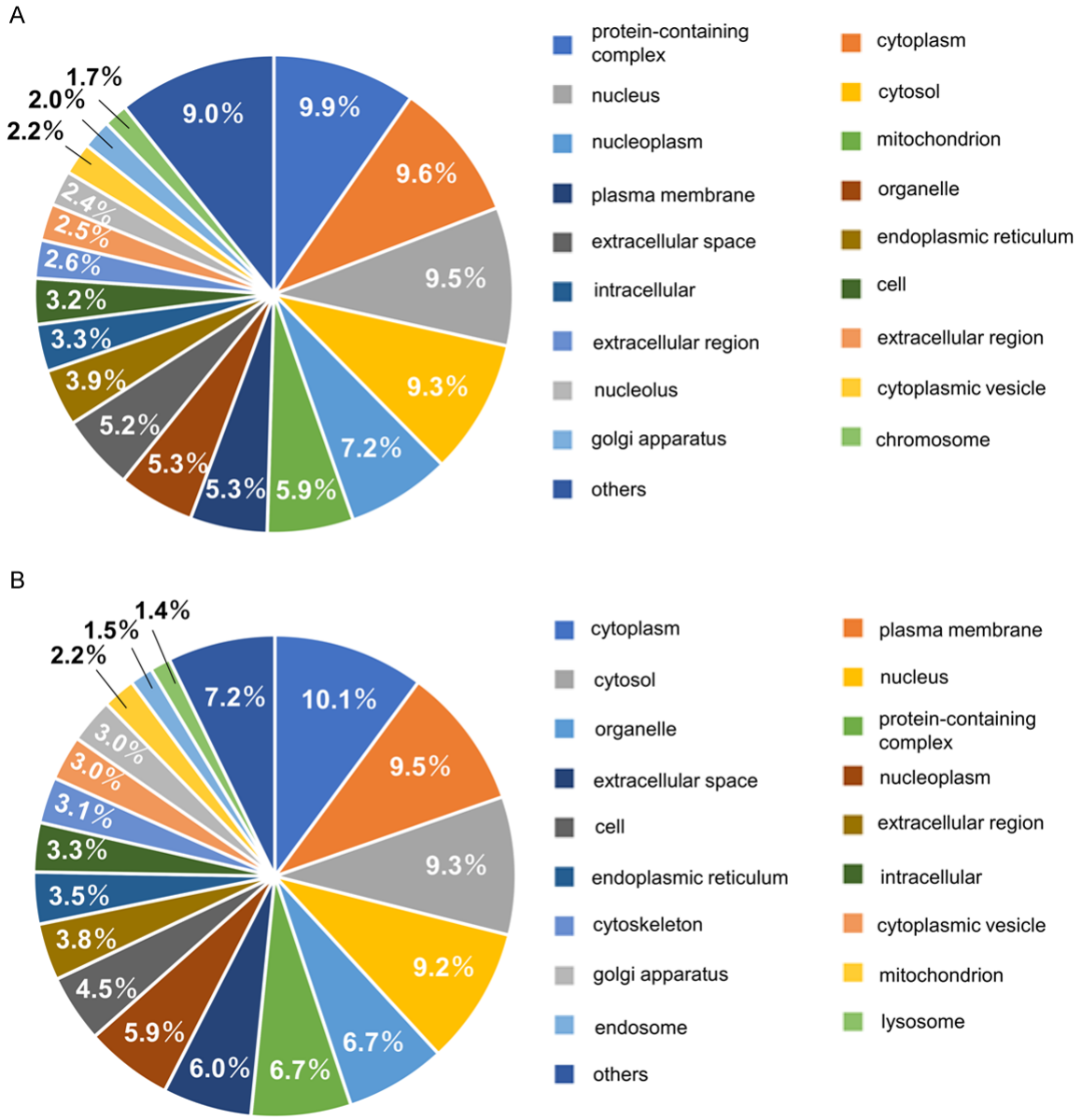

Figure 6. Gene Ontology enrichment analysis, focused on cellular components. A. Enriched Gene Ontology terms among upregulated (> 2-fold increase) genes in amoeboid-like CD44^{high} cells, compared with mesenchymal-like CD44^{high} cells. B. Enriched Gene Ontology terms among downregulated (< 0.5-fold decrease) genes in amoeboid-like CD44^{high} cells, compared with mesenchymal-like CD44^{high} cells.

6). With respect to molecular function, the most abundant GO term was ion binding in both upregulated and downregulated genes (**Figure 7**).

Discussion

Mesenchymal-like cancer cells can migrate through the surrounding tissue and ECM. Thus, it is likely that such plasticity with respect to cell motility is associated with tumor invasion and metastasis [17]. EMT is required for CSCs to undergo metastasis followed by mesenchymal-to-epithelial transition (MET) and to produce new tumor at sites of metastasis [2]. Thus, phenotypic plasticity is thought to be an important feature for CSCs. However, it has not been fully elucidated whether mesenchymal-like CD44^{high} OSCC cells can undergo further additional phenotypic change except for MET. Mesenchymal-like cells undergo mesenchymal to amoeboid transition (MAT) when

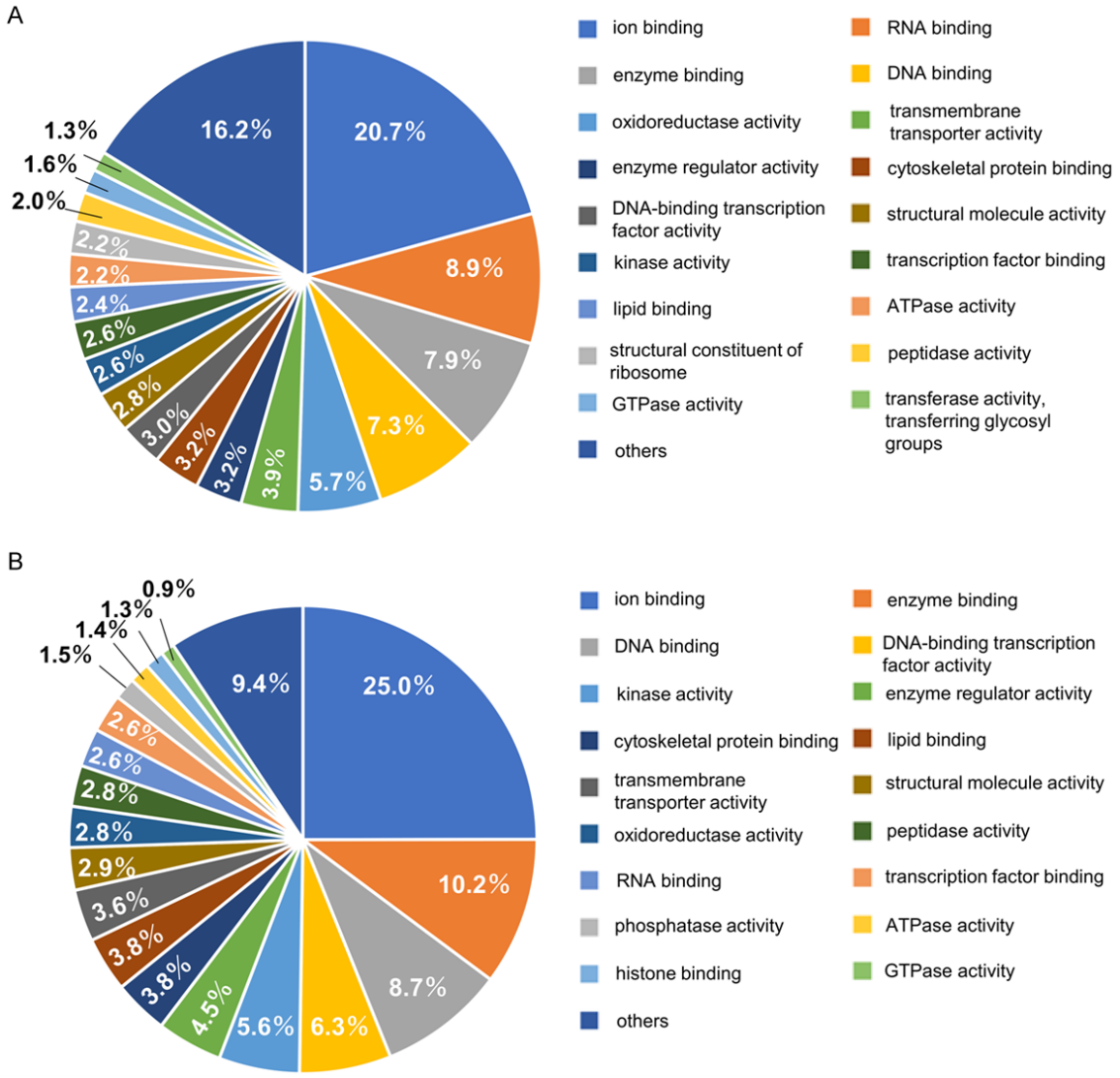

Figure 7. Gene Ontology enrichment analysis, focused on molecular functions. A. Enriched Gene Ontology terms among upregulated (> 2-fold increase) genes in amoeboid-like CD44^{high} cells, compared with mesenchymal-like CD44^{high} cells. B. Enriched Gene Ontology terms among downregulated (< 0.5-fold decrease) genes in amoeboid-like CD44^{high} cells, compared with mesenchymal-like CD44^{high} cells.

cells lose cell-ECM adhesion and increase actomyosin contractility [13]. Migrating mesenchymal-like cancer cells can alter cell motility, undergoing both MAT and amoeboid to mesenchymal transition [17]. In the present pilot study, CD44^{high} OM-1 cells underwent EMT followed by MAT when they were cultured on softer hydrogel. Importantly, CD44 expression did not change after undergoing MAT in CD44^{high} OM-1 cells, indicating that CSC property may be maintained in CD44^{high} OSCC cells after undergoing MAT. CD44^{high} OM-1 cells with CSC characteristics appear to have the ability to modify cell motility in response to ECM stiffness.

Amoeboid-like cells exhibited cellular blebs, which comprise dynamic protrusions that originate from the plasma membrane [18]. Rac, Rho, and Cdc42 are Ras-related GTP-binding proteins that regulate the assembly and organization of the actin cytoskeleton [19]. The Rho/ROCK signaling pathway plays a key role in regulation of actomyosin contractility in amoeboid-like cancer cells [20]; amoeboid-like cells can move through gaps in the ECM without causing ECM degradation or ECM-cell attachment [21]. Conversely, the occurrence of EMT is dependent on ECM degradation and remodeling [21]. Thus, MAT may be involved in cancer cell invasion, as well as EMT in OSCC.

Vimentin is known as the major intermediate filament and an important canonical marker of EMT [22]. Vimentin is extensively involved in the regulation of signal transduction, as well as maintenance of cellular structural integrity [23]. In addition, vimentin is reportedly involved in the regulation of differentiation markers, such as involucrin, filaggrin, and loricrin, in oral cancers [24]. Thus, vimentin may be vital for the maintenance of CSC properties through regulation of cell signaling pathways in OSCC cells [6]. In the present study, vimentin mRNA expression levels showed greater enhancement in epithelial-like CD44^{high} cells, compared with levels in mesenchymal-like CD44^{high} cells. Further experiments are needed to clarify the effect of matrix stiffness and type of ECM (e.g., collagen, laminin, or fibronectin) on the regulation of vimentin expression.

The results of microarray analysis suggested that signal transduction, biosynthetic processes, anatomical structure development, and cellular nitrogen compound metabolic process-associated genes may be associated with MAT in CD44^{high} OSCC cells. Importantly, cofilin, an intracellular actin-modulating protein, was highly expressed in amoeboid-like CD44^{high} cells. Cofilin has been identified as an effector of TGF-β signaling in human prostate cancer cells and is essential for growth and homeostasis of protrusions in amoeboid metastatic tumor cells [25, 26]. In addition, cofilin reportedly contributes to OSCC invasive capacity [27]. Collectively, these results highlight an important role for cofilin in the invasion and metastatic abilities of amoeboid-like cancer cells.

In summary, CD44^{high} OM-1 cells underwent MAT when cultured on laminin-coated softer hydrogel. Our observations suggest that phenotypic plasticity is a key characteristic of OSCC CSCs. Additionally, cofilin may play an important role in MAT in CD44^{high} OSCC cells. Further studies are needed to clarify the relationship between cofilin and invasion ability in amoeboid-like CD44^{high} OSCC cells.

Acknowledgements

This work was supported by a Grant-in-aid for Scientific Research (C) (No. 17K11837) from the Japanese Ministry of Education, Culture, Sports, and Technology.

Disclosure of conflict of interest

None.

Address correspondence to: Hideo Shigeishi, Department of Public Oral Health, Program of Oral Health Sciences, Graduate School of Biomedical and Health Sciences, Hiroshima University, 1-2-3 Kasumi, Minami-ku, Hiroshima 734-8553, Japan. Tel: +81-82-257-5945; Fax: +81-82-257-5945; E-mail: shige@hiroshima-u.ac.jp

References

[1] Prince ME, Sivanandan R, Kaczorowski A, Wolf GT, Kaplan MJ, Dalerba P, Weissman IL, Clarke MF and Ailles LE. Identification of a subpopulation of cells with cancer stem cell properties in head and neck squamous cell carcinoma. Proc Natl Acad Sci U S A 2007; 104: 973-978.

[2] Biddle A, Liang X, Gammon L, Fazil B, Harper LJ, Emich H, Costea DE and Mackenzie IC. Cancer stem cells in squamous cell carcinoma switch between two distinct phenotypes that are preferentially migratory or proliferative. Cancer Res 2011; 71: 5317-5326.

[3] Shigeishi H, Biddle A, Gammon L, Rodini CO, Yamasaki M, Seino S, Sugiyama M, Takechi M and Mackenzie IC. Elevation in 5-FU-induced apoptosis in head and neck cancer stem cells by a combination of CDHP and GSK3β inhibitors. J Oral Pathol Med 2015; 44: 201-207.

[4] Hashikata M, Shigeishi H, Okui G, Yamamoto K, Tobiume K, Seino S, Uetsuki R, Kato D, Ishioka Y, Ono S, Ohta K, Higashikawa K, Sugiyama M and Takechi M. Snail-induced CD44^{high} cells in HNSCC with high ABC transporter capacity exhibit potent resistance to cisplatin and docetaxel. Int J Clin Exp Pathol 2016; 9: 7908-7918.

[5] Shigeishi H, Hashikata M, Yokoyama S, Sakuma M, Murozumi H, Kato H, Rahman MZ, Seino S, Ishioka Y, Ohta K, Takechi M and Sugiyama M. CD44high/ESAlow squamous cell carcinoma cell-derived prostaglandin E2 confers resistance to 5-fluorouracil-induced apoptosis in CD44high/ESAhigh cells. Int J Clin Exp Pathol 2018; 11: 2356-2363.

[6] Seino S, Shigeishi H, Hashikata M, Higashikawa K, Tobiume K, Uetsuki R, Ishida Y, Sasaki K, Naruse T, Rahman MZ, Ono S, Simasue H, Ohta K, Sugiyama M and Takechi M. CD44(high)/ALDH1(high) head and neck squamous cell carcinoma cells exhibit mesenchymal characteristics and GSK3β-dependent cancer stem cell properties. J Oral Pathol Med 2016; 45: 180-188.

[7] Shigeishi H, Biddle A, Gammon L, Emich H, Rodini CO, Gemenetzidis E, Fazil B, Sugiyama M, Kamata N and Mackenzie IC. Maintenance of stem cell self-renewal in head and neck cancers requires actions of GSK3β influenced by CD44 and RHAMM. Stem Cells 2013; 31: 2073-2083.
[8] Northcott JM, Dean IS, Mouw JK and Weaver VM. Feeling stress: the mechanics of cancer progression and aggression. Front Cell Dev Biol 2018; 6: 17.
[9] Desgrosellier JS and Cheresh DA. Integrins in cancer: biological implications and therapeutic opportunities. Nat Rev Cancer 2010; 10: 9-22.
[10] Schwartz MA and DeSimone DW. Cell adhesion receptors in mechanotransduction. Curr Opin Cell Biol 2008; 20: 551-556.
[11] Löffek S, Franzke CW and Helfrich I. Tension in cancer. Int J Mol Sci 2016; 17.
[12] Barcus CE, Keely PJ, Eliceiri KW and Schuler LA. Stiff collagen matrices increase tumorigenic prolactin signaling in breast cancer cells. J Biol Chem 2013; 288: 12722-12732.
[13] Sahai E and Marshall CJ. Differing modes of tumour cell invasion have distinct requirements for Rho/ROCK signalling and extracellular proteolysis. Nat Cell Biol 2003; 5: 711-719.
[14] Berton S, Belletti B, Wolf K, Canzonieri V, Lovat F, Vecchione A, Colombatti A, Friedl P and Baldassarre G. The tumor suppressor functions of p27(kip1) include control of the mesenchymal/amoeboid transition. Mol Cell Biol 2009; 29: 5031-5045.
[15] Miyazaki K. Laminin-5 (laminin-332): unique biological activity and role in tumor growth and invasion. Cancer Sci 2006; 97: 91-98.
[16] Huang da W, Sherman BT and Lempicki RA. Systematic and integrative analysis of large gene lists using DAVID bioinformatics resources. Nat Protoc 2009; 4: 44-57.
[17] Gandalovičová A, Vomastek T, Rosel D and Brábek J. Cell polarity signaling in the plasticity of cancer cell invasiveness. Oncotarget 2016; 7: 25022-25049.
[18] Lorentzen A, Bamber J, Sadok A, Elson-Schwab I and Marshall CJ. An ezrin-rich, rigid uropod-like structure directs movement of amoeboid blebbing cells. J Cell Sci 2011; 124: 1256-1267.
[19] Tapon N and Hall A. Rho, Rac and Cdc42 GTPases regulate the organization of the actin cytoskeleton. Curr Opin Cell Biol 1997; 9: 86-92.
[20] Parri M and Chiarugi P. Rac and Rho GTPases in cancer cell motility control. Cell Commun Signal 2010; 8: 23.
[21] Panková K, Rösel D, Novotný M and Brábek J. The molecular mechanisms of transition between mesenchymal and amoeboid invasiveness in tumor cells. Cell Mol Life Sci 2010; 67: 63-71.
[22] Ivaska J. Vimentin: central hub in EMT induction? Small GTPases 2011; 2: 51-53.
[23] Danielsson F, Peterson MK, Caldeira Araújo H, Lautenschläger F and Gad AKB. Vimentin diversity in health and disease. Cells 2018; 7; E147.
[24] Dmello C, Sawant S, Alam H, Gangadaran P, Mogre S, Tiwari R, D'Souza Z, Narkar M, Thorat R, Patil K, Chaukar D, Kane S and Vaidya M. Vimentin regulates differentiation switch via modulation of keratin 14 levels and their expression together correlates with poor prognosis in oral cancer patients. PLoS One 2017; 12: e0172559.
[25] Zhu B, Fukada K, Zhu H and Kyprianou N. Prohibitin and cofilin are intracellular effectors of transforming growth factor beta signaling in human prostate cancer cells. Cancer Res 2006; 66: 8640-8647.
[26] Sidani M, Wessels D, Mouneimne G, Ghosh M, Goswami S, Sarmiento C, Wang W, Kuhl S, El-Sibai M, Backer JM, Eddy R, Soll D and Condeelis J. Cofilin determines the migration behavior and turning frequency of metastatic cancer cells. J Cell Biol 2007; 179: 777-791.
[27] Polachini GM, Sobral LM, Mercante AM, Paes-Leme AF, Xavier FC, Henrique T, Guimarães DM, Vidotto A, Fukuyama EE, Góis-Filho JF, Cury PM, Curioni OA, Michaluart P Jr, Silva AM, Wünsch-Filho V, Nunes FD, Leopoldino AM and Tajara EH. Proteomic approaches identify members of cofilin pathway involved in oral tumorigenesis. PLoS One 2012; 7: e50517.